Dynamics of Packed-Bed Reactors Loaded with Oxide Catalysts

The lattice of an oxide catalyst can act as a reservoir for oxygen, storing and releasing it for oxidation reactions at the catalyst surface under appropriate transient conditions. The implication of this oxygen storage property on the dynamic response characteristics of packed-bed reactors loaded with oxide catalysts has been investigated through an experimental study of 2-butene oxidation over vanadium oxide. Temperature profiles in a wall-cooled packed-bed reactor have been measured at steady state and following step changes in the feed butene concentration and in the feed gas flow rate. Thermal reactor runaway was observed experimentally for large step increases in the feed butene concentration following certain catalyst pretreatments. Gas flow rate step increases and less severe butene step increases resulted in the reactor temperature overshooting its final steady-state profile. These response characteristics are a direct consequence of the oxygen storage property of the vandaium oxide catalyst.

Ernest W. Arnold III
Sankaran Sundaresan
Department of Chemical Engineering
Princeton University
Princeton, NJ 08544

Introduction

Partial-oxidation reactions catalyzed by surfaces of transition-metal oxides are widely used to convert hydrocarbons into valuable chemical intermediates (Gates et al., 1979). Industrial partial oxidation processes include oxidation of naphthalene or *o*-xylene to phthalic anhydride over supported V_2O_5, V_2O_5-K_2SO_4, or V_2O_5-TiO_2, oxidation of C_4 hydrocarbons to maleic anhydride over vanadium phosphates, ammoxidation of propylene to acrylonitrile over bismuth molybdates, and others.

These selective oxidation reactions are often carried out in tubular arrays of wall-cooled fixed-bed reactors and the simulation of their steady-state performance has been a subject of many studies. It is necessary to understand the dynamic response of catalytic reactors to perturbations in the input variables in order to select proper control and start-up policies. The dynamic response of wall-cooled fixed-bed reactors has been studied by many researchers and a rich variety of complex characteristics have been analyzed, including attainment of different steady states depending on the initial conditions (Liu and Amundson, 1962; Padberg and Wicke, 1967), creeping reaction zones (Padberg and Wicke, 1967; Rhee et al., 1974; Puszynski and Hlavacek, 1980), and the wrong-way thermal response phenomenon (Boreskov and Slinko, 1965; Mehta et al., 1981). In most theoretical investigations of reactor dynamics, it is invariably assumed that the catalyst responds instantaneously to changes in the catalyst temperature and the gas phase composition immediately above the catalyst surface. The dynamics of the catalyst itself has been considered in only a few limited studies of reactor dynamics, such as those addressing catalyst deactivation, poisoning, or fouling (Ervin and Luss, 1970; Blaum, 1974), or self-sustained reaction rate oscillations (Razon and Schmitz, 1986).

The assumption of instantaneous response of a metal catalyst is often justifiable and such an assumption will not affect the qualitative structure of the reactor response in a profound way. However, such is not the case in the context of oxide catalysts used for oxidation reactions. For example, the transient overshoots in the rate of 2-butene oxidation in an isothermal differential reactor and pellet temperature overshoots in a nonisothermal single-pellet reactor following step increases in the 2-butene feed concentration were shown to be direct consequences of oxygen stored in a supported vanadium oxide catalyst (Arnold and Sundaresan, 1987).

The purpose of the present study is to examine the effect of lattice oxygen (storage) participation on the dynamic responses of a wall-cooled packed-bed reactor loaded with a metal oxide catalyst. The same model reaction, 2-butene oxidation over supported vanadium oxide, is used to study the temperature profiles of a wall-cooled packed-bed reactor under steady-state and transient operations. It will be shown that, following a step increase in the feed flow rate or feed butene concentration, an appreciable overshoot in the reactor hot spot temperature can

come about (sometimes leading to thermal runaway) and that this is a direct consequence of oxygen storage in this catalyst system.

Experimental System

Supported vanadium oxide catalyst was prepared by impregnating granules (~2 mm) of a γ-alumina support (surface area = 44 m^2/g) with an aqueous solution of ammonium metavanadate and oxalic acid, followed by drying at 375 K and calcination at 665 K. The vanadium oxide loading in this catalyst was estimated to be ~3% by weight.

This catalyst was packed in a 20 cm long bed around an axial thermowell (7 mm OD) in one leg of a Pyrex U-tube (20 mm ID). The catalyst bed was supported on and covered with glass beads of 3 mm dia. The other leg of the U-tube was filled with glass beads to facilitate preheating of the feed gases. The entire U-tube was placed in an aluminum split block that was surrounded by two separately controlled electical heating tapes and insulation. Two fine chromel-alumel thermocouples placed between the U-tube and the aluminum split block were used to control the two electrical heating tapes and maintain a nearly uniform reactor wall temperature. Seven thermocouples were placed at approximately 3 cm spacings in the axial thermowell.

Butene and dry air were metered separately and mixed to achieve the desired compositions. The flow rate of this mixture to the reactor was controlled by metering a portion of this mixture, while venting the remainder. Steady-state experiments in this packed-bed reactor consist of measuring the temperature profile of the catalyst bed at various feed gas flow rates, butene concentrations, and reactor wall (cooling) temperatures.

Two separate gas metering systems were used in conjunction with a four-way selector valve located close to the reactor inlet in the transient experiments where the changes in the reactor temperature profile were monitored following step changes in the feed butene concentrations (in air) and feed gas flow rate. Step changes in the feed and cooling temperatures were not possible in this reactor system.

The feed and effluent streams were analyzed by on-line gas chromatography. A side stream ran from the heated effluent line to a HP 5790 gas chromatograph where partial oxidation products were separated on a 2 m long Porapak QS column. After the reactor effluents passed through a water bubbler to trap the partial oxidation products, samples were injected (via a sampling loop) into two chromatographic columns in series: a 5 m long 30% bis-2-ethoxy ethyl sebacate column to resolve CO_2 and hydrocarbons, and a 4 m long 13X molecular sieve column to separate O_2, N_2, and CO.

Kinetic experiments were also carried out in a U-tube reactor (7 mm ID) housed inside an aluminum split block. One leg of the U-tube was filled with crushed catalyst pellets, while the other leg was filled with glass beads to facilitate preheating of the feed gases. Nearly isothermal conditions were achieved in the catalyst bed by using an axial glass rod (4 mm dia.) in the leg of the U-tube where the catalyst was loaded and also by diluting the catalyst with crushed glass beads.

Results

Examples of the steady-state temperature profiles measured in the wall-cooled reactor are shown in Figures 1a and 1b. Figure 1a shows the variation of the temperature profile with the

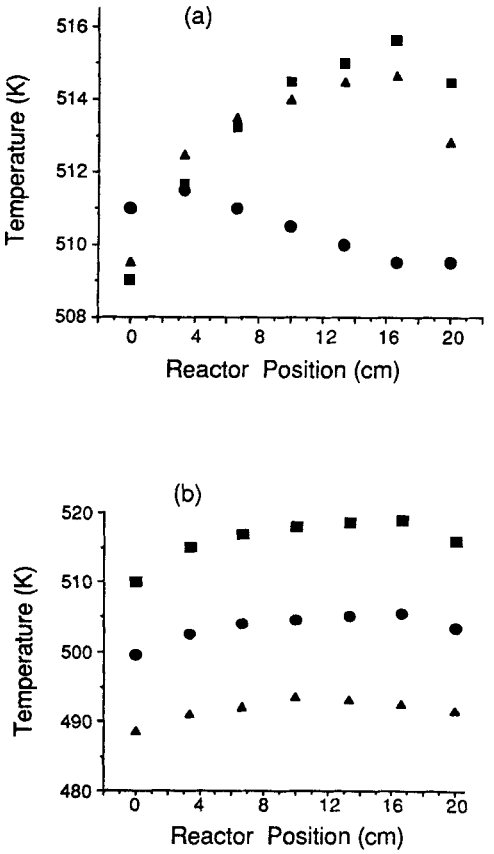

a. Effect of flow rate: ● = 25 mL/min; ▲ = 700 mL/min; ■ = 1,700 mL/min; T_w = 508 K; x_B = 0.0175
b. Effect of reactor wall temperature: ▲ = 488 K; ● = 498 K; ■ = 508 K; flow rate = 700 mL/min; x_B = 0.0175

Figure 1. Temperature profiles in wall-cooled reactor.

gas flow rate for a fixed butene concentration and reactor wall temperature. The variation with the reactor wall temperature is shown in Figure 1b. Butene conversions range from ~5 to ~100% for the temperatures profiles shown in Figures 1a and 1b. These steady-state temperature profiles were reproducible within ±1°C.

The hot spot temperatures measured in the reactor at different butene concentrations are presented in Figure 2 for two different wall temperatures and feed gas flow rates. Neither multiple steady states nor steady-state parametric sensitivity was observed for any butene concentrations (less than 2.0% butene in air, the lower limit of the explosive envelope) at the reactor wall temperatures (480–520 K) and gas flow rates (25–2000 mL/min) studied.

The transient temperature profiles of the catalyst bed following a step increase in the butene concentration (0.0 to 1.75% in air) are shown in Figures 3a and 3b for two different catalyst pretreatments. The seven temperatures measured at each time have been connected with lines to yield a rough reactor temperature profile. This concentration step increase represents a possible reactor start-up procedure. The initial temperature profile is flat and equal to that of the coolant (aluminum block) since there is no reaction taking place. For pretreatment in air, Figure 3a, the bed temperature rises rather uniformly at first following the concentration step increase. A distinct temperature peak develops by about 10 min. This spike moves down the reactor in

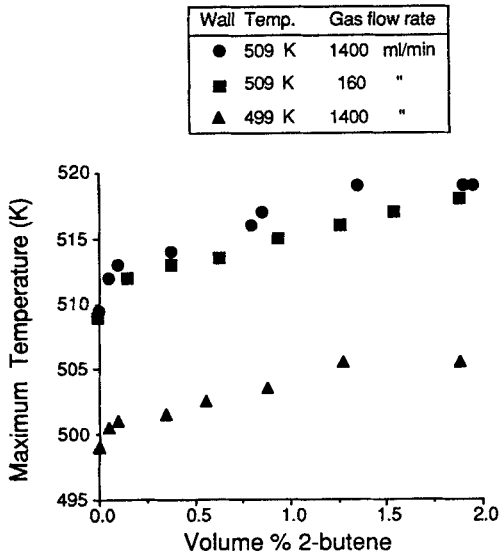

Figure 2. Reactor hot spot temperatures vs. feed butene concentration.

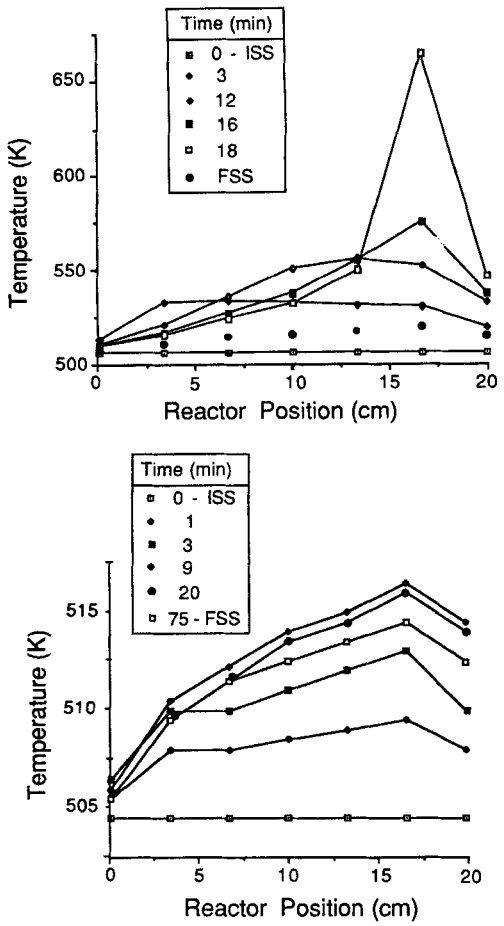

a. Catalyst pretreated 10.5 h in air
b. Catalyst pretreated in nitrogen

Figure 3. Transient temperature profiles following step increase in butene concentration, x_B = 0.0 to 0.0175.

T_w = 505 K; flow rate = 1,700 mL/min
ISS, initial steady state; FSS, final steady state

time, becoming taller and narrower. By 18 min, the hot spot temperature exceeded 650 K and was rising rapidly. At this time, the butene feed was cut off for safety reasons. The solid circles in Figure 3a represent the steady-state temperature profile measured at this feed gas flow rate, feed butene concentration (1.75%), and reactor wall temperature by following a transient procedure that avoided runaway. Even with the extreme transient temperature peak, the temperatures in the front of the catalyst bed had nearly attained their final steady-state values when the reactor had to be turned off.

The same initial steady-state temperature profile was observed after the nitrogen pretreatment, Figure 3b. Again, the bed temperature rose rather uniformly soon after the concentration step increase, but no large transient temperature peak was observed. The temperature reached its final steady-state profile in about 75 min. This final steady-state profile was identical to that measured previously for the 1.75% butene feed shown in Figure 3a.

Figure 4 shows the transient responses of the wall-cooled packed-bed reactor to this step increase (0.0 to 1.75%) in the butene concentration for several catalyst pretreatments in air and nitrogen. The time history of the measured reactor hot spot temperature is shown. The curves for the nitrogen and the 10.5 h air pretreatments are taken from the transient temperature profiles shown in Figures 3a and 3b. For the nitrogen pretreatment, the reactor hot spot exceeds its final steady-state value during the transient by only a few degrees Celsius. Thermal reactor runaway was observed following the same concentration step increase when the catalyst was pretreated in air for 10.5 h. For shorter air pretreatments, the reactor hot spot goes through a transient maximum before reaching its final steady-state value. The magnitude of the transient overshoot in the hot spot temperature increases with the length of time the catalyst was treated in air. The same final steady-state hot spot temperature (within 1°C) was observed regardless of the catalyst pretreatment.

The reactor conditions selected in Figure 4 were chosen to illustrate the extreme reactor responses that are possible following a step increase in the feed butene concentration for catalysts pretreated in air. Less severe concentration step increases can result in transient temperature overshoots—such as shown in Figure 4 for short time air pretreatments—and well-behaved final steady states will be attained. Three examples of tempera-

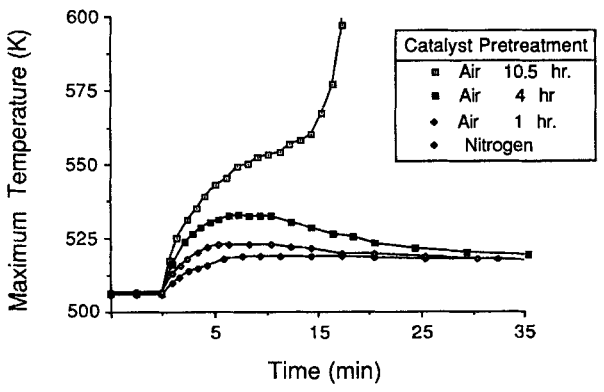

Figure 4. Time histories of reactor hot spot temperature following step increase in butene concentration, x_B = 0.0 to 0.0175.

T_w = 505 K; flow rate = 1,700 mL/min

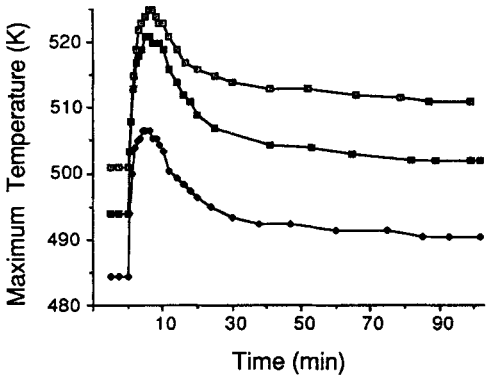

Figure 5. Time histories of hot spot temperatures for three butene step increases, x_B = 0.0 to x_{B2}.

□ x_{B2} = 0.0175; T_w = 501 K; flow rate = 400 mL/min
■ x_{B2} = 0.011; T_w = 494 K; flow rate = 1,700 mL/min
♦ x_{B2} = 0.011; T_w = 484 K; flow rate = 1,700 mL/min

ture overshoots without thermal runaway are shown in Figure 5 for different concentration step increases. In each case, the catalyst was pretreated overnight (10–16 h) in air.

The transient overshoot phenomena observed for the reactor hot spot temperature is not restricted to concentration step increases from an initial null butene concentration (air pretreatment). Figure 6 shows two transient temperature overshoots following concentration step increases (0.1 to 1.90%, 0.2 to 1.75%) at two different reactor temperatures. The magnitude of the temperature overshoot increases with the severity of the butene concentration step, as can be seen by comparing the last two figures. The largest temperature overshoot in Figure 6 was 5°C, while those in Figure 5 ranged from 14 to 19°C.

The variation of the measured reactor hot spot temperature under steady-state conditions with the gas flow rate is shown in Table 1. Although the hot spot temperature does not vary much with the gas flow rate (at least above 100 mL/min), the total butene conversion and the shape of the temperature profile both do. At low flow rates, the butene is almost entirely consumed, so the bed temperature rises to a maximum and falls back nearly to the wall (cooling) temperature. At high flow rates, the butene

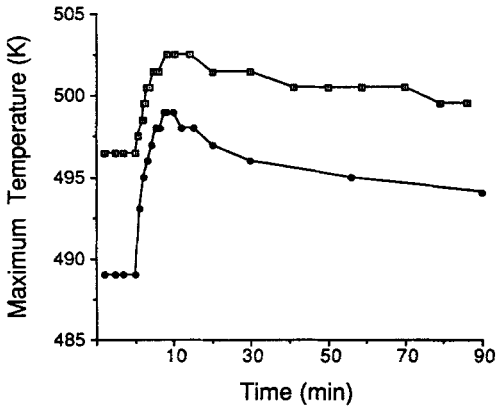

Figure 6. Transient hot spot temperature overshoots for step increases in butene volume fraction in feed from x_{B1} to x_{B2}

□ x_{B1} = 0.002; x_{B2} = 0.0175; T_w = 496 K; flow rate = 1,700 mL/min
● x_{B1} = 0.001; x_{B2} = 0.0190; T_w = 488 K; flow rate = 400 mL/min

Table 1. Variation of Hot Spot Temperature with Gas Flow Rate

u mL/min	Hot Spot Temp., K
25	511.0
90	513.5
160	514.0
700	515.5
1,700	515.5

x_B = 0.018; T_o = T_w = 508 K

concentration is nearly uniform throughout the reactor and the temperature profile has a flat broad hot spot.

The transient response of the reactor hot spot temperature following a step increase in the feed gas flow rate is shown in Figure 7. A hot spot temperature overshoot similar to those observed following concentration step increases was measured.

Product distribution (selectivity) measurements were carried out under steady-state and transient reactor operations. The observed products can be split into two groups: partial oxidation products (maleic anhydride, furan, crotonaldehyde and acetic acid), and total oxidation products (carbon oxides). Water is produced as a by-product for both total and partial oxidation of the 2-butene. Following a step increase in the butene concentration for several different catalyst pretreatments (transient temperature responses shown in Figure 4), the partial oxidation selectivity did not vary appreciably with time (30 ± 3%) even though the butene conversions varied by a factor of four. The partial oxidation selectivity is defined as the percentage of the 2-butene consumed which formed the partial oxidation products. Selectivities in this range (30 ± 3%) were also observed in the wall-cooled reactor at steady-state and also in an isothermal differential reactor loaded with crushed catalyst pellets, which was used to obtain the steady-state kinetic data. However, the partial oxidation selectivity was significantly lower when reactor runaway, such as that shown in Figure 3a, occurred. This drop in selectivity was due to the high butene conversions that accompany these extreme temperature profiles. At high conversions, the further oxidation of the partially oxygenated products is not negligible and accounts for the observed decline in partial oxida-

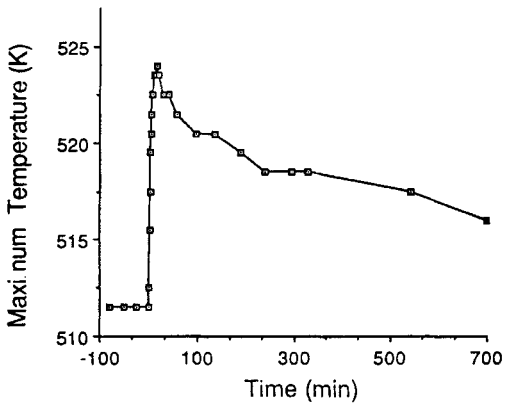

Figure 7. Transient response of observed reactor hot spot temperature following step increase in gas flow rate, 25 to 700 mL/min.

T_w = 508 K; x_B = 0.018

tion selectivity. The selectivity 3 min after the butene step change was 29.0%; quite typical for this system, while at 17 min (the onset of reactor runaway), the selectivity had declined to about 5.0%. Such selectivity loss upon thermal runaway is quite well known in partial-oxidation reactors.

Discussion

Although the steady-state results obtained in the fixed-bed reactor experiments, Figures 1 and 2, are rather mundane, the transient results speak for the complexity of oxide catalysts. Figures 3a, 3b, and 4 clearly illustrate the importance of the catalyst bed history for the resulting transient characteristics. We believe that this history dependence is intimately linked with the ability of metal oxide catalysts to store oxygen in its bulk (lattice) and release it for reactions at the catalyst surface under appropriate conditions. This is seen in Figures 3a, 3b, and 4, which show that the oxidation state of the catalyst can have a pronounced influence on the dynamic responses of the reactor. Oxidizing pretreatments replenish the lattice oxygen, which can be detrimental to the transient response characteristics of the catalyst, Figure 3a. Nitrogen pretreatment does not replenish the lattice oxygen, thereby eliminating the adverse response characteristics, Figure 3b. The concept that oxygen can be stored in metal oxide catalysts and that it can participate in reactions on the catalyst surface is not new (Bradzil et al., 1980; Hodnett and Delmon, 1984; Buchanan and Sundaresan, 1986; Breckner et al., 1987). But the possible consequences of such participation on the reactor response characteristics do not appear to have been explored in a systematic way.

As discussed elsewhere (Arnold and Sundaresan, 1987), since the selectivity of the reaction system was essentially invariant (except after runaway had set in), the reaction rates in this multireaction network may be modeled as a single overall reaction:

$$C_4H_8 + \frac{n}{2}O_2 \rightarrow \text{Products}$$

Using a redox model representation (Mars and van Krevlen, 1954), we can write

$$C_4H_8 + nS\text{-}O \xrightarrow{k_1} \text{Products} + nS\text{-} \qquad \text{(R1)}$$

$$\frac{1}{2}O_2 + S\text{-} \xrightarrow{k_2} S\text{-}O \qquad \text{(R2)}$$

where S-O and S- represent oxidized and reduced surface sites, respectively. The butene oxidation reaction is not nth order as it might appear because reaction R1 is a combination of several elementary steps and the reaction rate is determined by the first S-O attack. The reoxidation reaction is represented in the form shown in reaction R2, instead of

$$O_2 + 2S\text{-} \xrightarrow{k_2} 2S\text{-}O$$

purely for reasons of algebraic simplicity. At steady state, the above reactions proceed at equal rates so that $r_1 = r_2$, where

$$r_1 = nk_1C_B[S\text{-}O], \quad r_2 = k_2C_{O_2}^{1/2}[S\text{-}]$$

Further, as $[S\text{-}] + [S\text{-}O] = 1$, we can write the steady-state rate of butane oxidation as

$$k_1k_2C_BC_{O_2}^{1/2}/(nk_1C_B + k_2C_{O_2}^{1/2})$$

The steady-state kinetic data obtained with the crushed catalyst pellets (in the differential reactor experiments in the temperature range 493–552 K) could be correlated quite satisfactorily with the above functional form. From the experimental data on product distribution, it was estimated that $n = 8.6$ and $(-\Delta H_1) + n(-\Delta H_2) = 1{,}658$ kJ/gmol. A least-squares regression of the steady-state kinetic data was used to estimate k_1 and $k_2C_{O_2}^{1/2}$ presented in Table 2. As the oxygen volume fraction was close to 0.21 in most of our experiments, we could not verify whether the one-half power dependence on C_{O_2} was correct. However, this is not significant for the purpose of our study.

In order that the oxygen in the catalyst lattice (bulk) participate in the reaction processes occurring in the surface layer, we must allow for the exchange of oxygen between the surface layer and the subsurface region in the catalyst lattice,

$$S\text{-}O + L\text{-} \underset{k_{-3}}{\overset{k_3}{\rightleftharpoons}} S\text{-} + L\text{-}O \qquad \text{(R3)}$$

where L-O and L- respectively denote oxygen in the catalyst lattice that can be easily removed and an oxygen vacancy in the catalyst lattice. In addition to the exchange reaction, R3, an elaborate model for the participation of the oxygen in the catalyst lattice should also consider the details of the process by which the oxygen diffuses in the catalyst lattice. In an earlier paper (Arnold and Sundaresan, 1987), we treated the catalyst bulk through a lumped model (for the sake of simplicity) as a reservoir for oxygen. While such a treatment of the catalyst bulk is very simplistic, it was found to be adequate to capture the qualitative features observed in a single-pellet reactor. In the present work, this lumped model for the lattice oxygen dynamics has been combined with a simple model for a wall-cooled packed-bed reactor, namely a one-dimensional pseudohomoge-

Table 2. Kinetic and Reactor Parameters

ρ_s	1.0×10^3 kg/m^3
ρ_f	0.63 kg/m^3
c_{ps}	0.96 kJ/kg · K
c_{pf}	1.05 kJ/kg · K
C_p	1.05×10^3 kJ/m^3 · K
$k_1(T)$	$4.37 \times 10^{10} \exp(-15{,}800/T)$ m^3/kg cat · s
$k_2(T)C_{O_2}^{1/2}$	$1.265 \times 10^{10} \exp(-16{,}000/T)$ mol/kg cat · s
k_{-3}	3.0×10^{-2} mol/kg cat · s
K_3	$10 = k_3/k_{-3}$
n	8.6
$(-\Delta H_1)$	1,650 kJ/mol
$(-\Delta H_2)$	8.40 kJ/mol
$(-\Delta H_3)$	0 kJ/mol
E_1	−131 kJ/mol
E_2	−133 kJ/mol
E_3	0 kJ/mol
W_cC_o	5.5 mol O_2/kg cat
U_h	0.167 kJ/m^2 · s · K
d_t	0.015 m
λ_{ea}	4×10^{-5} kJ/m · s · K
x_B	0.0–0.02
T_o, T_w	520–650 K
u	0.01 – 4.0 m/s

neous model. The transient responses of this reactor to step changes in the concentration, inlet temperature, and feed gas flow rate are calculated both with and without the lattice oxygen exchange reaction. The purpose of these simulations is not to seek quantitative comparisons with the experimental data (as a one-dimensional model is too simplistic to describe our experimental reactor quantitatively), but to examine whether the participation of lattice oxygen is a plausible explanation for the qualitative features observed experimentally.

The lumped model for lattice oxygen participation discussed in the previous study (Arnold and Sundaresan, 1987) is described by

$$M_s \frac{d}{dt}[S\text{-}O] = -nk_1 C_B[S\text{-}O] + k_2 C_{O_2}^{1/2} + k_{-3}[L\text{-}O][S\text{-}] - k_3[L\text{-}][S\text{-}O]$$

$$W_c C_o \frac{d}{dt}[L\text{-}O] = k_3[L\text{-}][S\text{-}O] - k_{-3}[L\text{-}O][S\text{-}] = r_3$$

$$[L\text{-}] + [L\text{-}O] = 1$$

where all rate constants have the usual Arrhenius form. Here, W_c denotes the weight fraction of active catalyst material (vanadium oxide) in the supported catalyst and C_o is the amount of easily removable oxygen in the catalyst per unit mass of vanadium oxide. It is well known that V_2O_5 can easily be reduced to V_2O_4 and with somewhat less ease to V_2O_3. Further reduction is generally believed to be very difficult. Thus, we assume that two atoms of oxygen can be removed per molecule of V_2O_5. Therefore, $C_o \sim 0.011$ mol of O per gram of V_2O_5. The oxygen storage capacity in the catalyst bulk is far greater than that in the surface layer for the model system studied here. Hence, one may assume a quasisteady state for $[S\text{-}O]$. The values of k_3 and $K_3 = k_3/k_{-3}$ were estimated by comparing model predictions with the transient reaction rate data obtained in the isothermal differential reactor using crushed catalyst pellets (Arnold, 1988). The heats of reactions R2 and R3 have been estimated from single-pellet reactor experiments, as described in our previous study (Arnold and Sundaresan, 1987). All these parameter values are listed in Table 2.

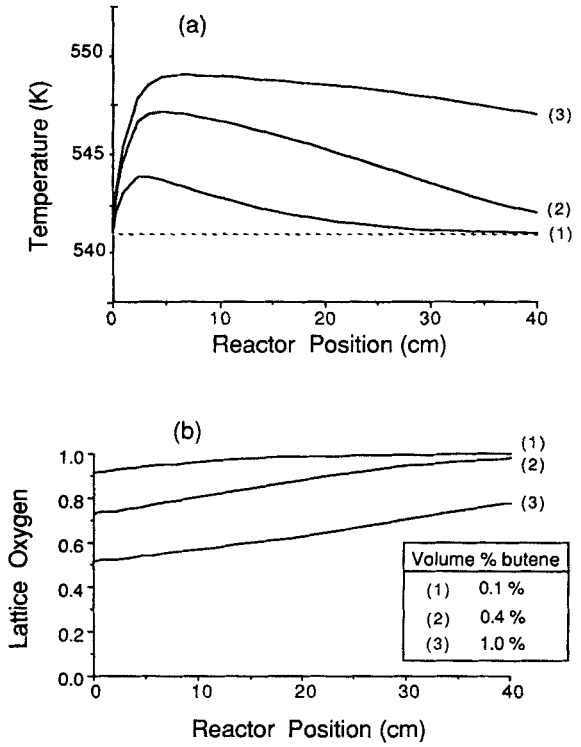

a. Temperature profiles
b. Dimensionless lattice oxygen profiles

Figure 8. Steady-state trends predicted by reactor model for three butene feed levels.

$T_o = T_w = 541$ K; flow rate = 50 cm/s

The pseudosteady approximation has been assumed for the mass balance in the wall-cooled reactor model as the characteristic time for mass transport is much less than that for energy transport in the present context. Neglecting axial dispersion of mass yields the following mass balance:

$$-u\frac{\partial C_B}{\partial z} = \rho_s r_1$$

Axial energy dispersion has been included in the energy balance to avoid the possibility of infinitely steep transient temperature spikes (Mehta et al., 1981). The following energy balance and boundary conditions were used:

$$C_p \frac{\partial T}{\partial t} = \lambda_{ea}\frac{\partial^2 T}{\partial z^2} - u\rho_f c_{pf}\frac{\partial T}{\partial z} - \frac{4U_h}{d_t}(T - T_w) + \rho_s[r_1(-\Delta H_1) + r_2(-\Delta H_2) + r_3(-\Delta H_3)]$$

$$u\rho_f c_{pf}[T_o - T(0)] = -\lambda_{ea}\frac{\partial T}{\partial z} \quad \text{at } z = 0$$

$$\frac{\partial T}{\partial z} = 0 \quad \text{at } z = L$$

The parameters used in this wall-cooled packed-bed reactor model are also shown in Table 2. Parameter values were chosen to closely simulate a typical commercial-scale oxidation reactor. A Hermite interpolation technique was used to discretize the wall-cooled reactor model. The details of the numerical scheme are described elsewhere (Arnold, 1988).

The steady-state temperature profiles predicted for three butene concentrations at a fixed reactor (coolant and inlet) temperature and gas flow rate are shown in Figure 8a. The corresponding lattice oxygen (dimensionless) profiles are shown in Figure 8b. Notice that a large amount of lattice oxygen must be released following a step increase in the butene concentration from 0.1 to 0.4% or to 1.0% before the final steady state is reached. Previous work with this lattice oxygen exchange model (Arnold and Sundaresan, 1987) has shown that the release of lattice oxygen is accompanied by an overshoot in the rate of butene oxidation. This reaction rate overshoot can lead to temperature overshoot, sometimes resulting in runaway, as shown below.

The transient response of the reactor hot spot temperature predicted following a step increase in the butene concentration is shown in Figure 9 both with and without lattice oxygen participation. A butene step increase from 0.0 to 1.0% has been modeled to imitate a possible reactor start-up procedure. Without lattice oxygen participation, the hot spot temperature increases monotonically from its initial steady-state value to that of the

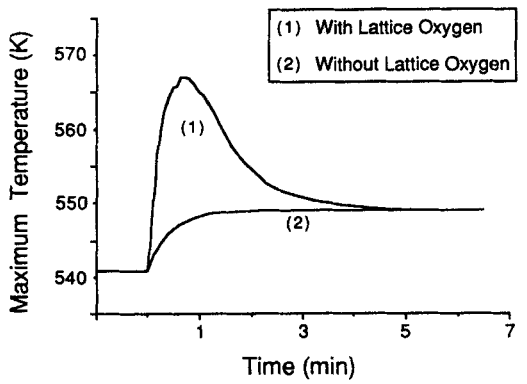

Figure 9. Predicted transient responses of reactor hot spot temperature following butene step increase, x_B = 0.0 to 0.01.
$T_o = T_w$ = 541 K; flow rate = 50 cm/s

final steady state, which is reached in about 2 min. The transient hot spot temperature goes through a sharp maximum with lattice oxygen participation. The final steady-state temperature profile was reached in about 5 min and was identical to that predicted without lattice oxygen. For this butene step increase, the maximum transient temperature with lattice oxygen exceeds that predicted without lattice oxygen participation by about 20°C.

The effect of the final butene concentration on the maximum transient temperature predicted following a step increase from pure air (0.0% butene) is shown in Figure 10, both with and without lattice oxygen participation. The two points at 1.0% are the maximum temperatures from the curves in Figure 9. It so happens that the maximum hot spot temperature reached during transients in the absence of lattice oxygen participation was identical to that corresponding to the final steady-state locus. Thus, the difference between the two curves in Figure 10 is the transient temperature overshoot induced by the lattice oxygen participation, which increases with the butene step size. For final butene concentrations above 1.24%, the wall-cooled packed-bed model predicts severe hot spot temperatures during the transients—in other words, reactor runaway, with lattice oxygen participation following a step increase from 0.0%. However, it should be noted that well-behaved steady-state temperature profiles do indeed exist for butene concentrations well above 1.24% (at least to 2.0%, the explosive limit). Thus, the participation of lattice oxygen can introduce a dynamic parametric sensitivity.

Figure 11 shows the maximum transient reactor temperature predicted with lattice oxygen participation at five different reactor temperatures following butene step increases from 0%. Thermal reactor runaway was predicted for sufficiently large butene step increases for all but the lowest reactor temperature. The butene step size that can be tolerated by the reactor (i.e., no runaway) decreases with increasing reactor temperature.

The above simulation results clearly point out that the lattice oxygen participation can lead to temperature overshoots, and sometimes thermal runaway, following step increases in feed butene concentration. The features of the transient reactor responses are qualitatively similar to those observed experimentally. This suggests that the participation of the lattice oxygen under transient conditions is indeed a plausible explanation for our experimental observations.

The fact that the participation of lattice oxygen introduces a dynamic parametric sensitivity is quite significant. To illustrate this, let us consider the wall heat transfer coefficient U_h, which is an important parameter when designing and operating wall-cooled oxidation reactors. Figure 12 shows the reactor sensitivity with U_h for three operating conditions. The maximum reactor temperature is plotted against U_h. Steady-state simulations with a 1.0% butene feed, curve *1*, predict parametric sensitivity just below $U_h = 0.100$ kJ/m^2 · K · s. This would be the critical design value of U_h based on steady-state reactor performance.

We know now that transient temperature overshoots can occur in reactors loaded with oxide catalysts following step increases in the feed butene concentration. The other two curves in Figure 12 show the maximum transient temperatures predicted for two possible reactor start-up procedures (with lattice oxygen): curve *3* a step increase from 0.0 to 1.0% butene, and curve *2* a step increase from 0.0 to 0.4% followed by a subsequent step to 1.0% butene after the intermediate steady state had been attained. Dynamic parametric sensitivity is seen for

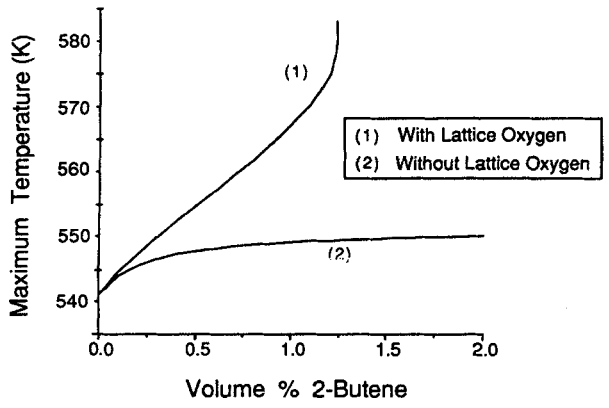

Figure 10. Predicted maximum transient temperatures vs. final butene concentration following step increase from x_B = 0.0.
$T_o = T_w$ = 541 K; flow rate = 50 cm/s

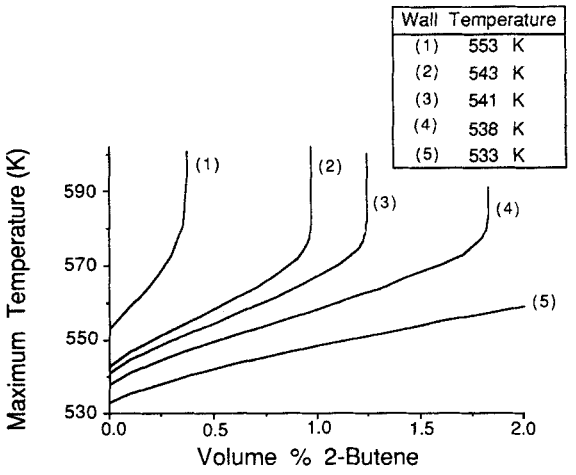

Figure 11. Predicted maximum transient temperatures vs. final butene concentration following step increase from x_B = 0.0.
Flow rate = 50 cm/s

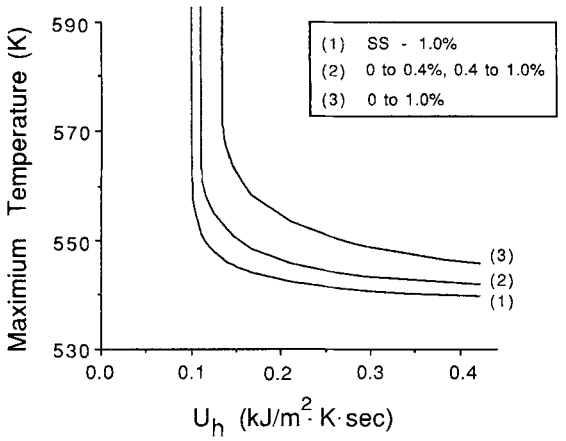

Figure 12. Maximum reactor temperature as a function of wall heat transfer coefficient under steady state and two start-up operations.

$x_B = 0.01$; $T_w = 538$ K; flow rate = 50 cm/s

these two start-up procedures at values of U_h significantly larger than 0.100, the value for steady-state parametric sensitivity. If this oxidation reactor were designed to operate properly under a 0.0 to 1.0% butene start-up procedure, the critical design value of U_h would be about 0.134.

Figure 13 shows the transient reactor responses predicted for a step change in the feed gas flow rate both with and without lattice oxygen participation. A significant temperature overshoot (15 K) is predicted with lattice oxygen while a very small overshoot (0.3 K) was predicted without lattice oxygen participation. Physically, for small flow rates, the butene is consumed early in the reactor and the oxide catalyst toward the back of the reactor is in a highly oxidized state. An increase in the flow rate brings butene in contact with this highly oxidized catalyst, leading to increased transient reaction rates. This is quite similar to the scenario following an increase in feed butene concentration.

The effect of lattice oxygen participation on the reactor dynamics following step changes in the reactor inlet temperature was also examined in our simulations. A wrong-way thermal response phenomenon is a well-known dynamic response of a nonisothermal, fixed-bed catalytic reactor following a step decrease in the inlet temperature (Boreskov and Slinko, 1965; Mehta et al., 1981). The different propagation speeds of mass

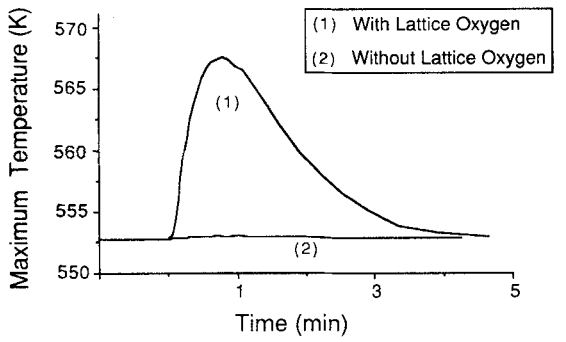

Figure 13. Predicted transient temperature response following step increase in gas flow rate, 10 to 100 cm/s

$T_o = T_w = 543$ K; $x_B = 0.01$

and energy waves in the reactor are responsible for a traveling temperature peak that can greatly exceed the maximum temperatures of the initial and final steady states. This wrong-way response can arise even in the absence of any complex catalyst characteristics, such as oxygen storage discussed in the present study. Accordingly, wrong-way response leading to runaway following a step decrease in feed temperature was observed in some of our simulations even in the absence of lattice oxygen participation. We simply note that including the lattice oxygen participation in our simulations resulted in much more aggravated wrong-way responses. Additional details can be found elsewhere (Arnold, 1988).

Conclusions

Although metal oxide catalysts are widely used in industry to carry out a variety of oxidation reactions, little has been published on the dynamic characteristics of these catalysts. The ability of an oxide catalyst to store oxygen in its bulk (lattice) and release it for reactions at the catalyst surface under appropriate conditions plays an important role in the dynamic response characteristics of this catalyst. Our experimental study of 2-butene oxidation over a supported vanadium oxide catalyst as a model reaction system revealed that this oxygen storage capacity of an oxide catalyst can give rise to a reaction rate overshoot following a step increase in the hydrocarbon concentration.

Under nonisothermal conditions, such a reaction rate overshoot can lead to a temperature overshoot. We have illustrated both experimentally and through reactor simulations that oxidation reactors loaded with metal oxide catalysts are less stable under certain dynamic operating conditions than under steady-state operation and that the release of lattice oxygen stored in metal oxide catalysts is at least in part responsible for this dynamic parametric sensitivity. Lattice oxygen has been shown to cause temperature overshoots following step increases in the feed concentration and the feed gas flow rate, and to exacerbate the wrong-way response following a step decrease in the reactor inlet temperature. Reactor runaway can result during any of these three dynamic conditions, even though well-behaved final steady states exist in each case. Any of these three situations may occur during start-up or operation of an oxidation reactor. Thus, the effects of lattice oxygen participation must be considered when determining proper start-up and control policies for oxidation reactors loaded with metal oxide catalysts.

Acknowledgment

We wish to thank the National Science Foundation, Grant No. CBT-8405132, and the Shell Foundation for financial support of this work.

Notation

C_B, C_{O_2} = concentration of butene, oxygen
C_o = removable oxygen per mol V_2O_5
C_p = bulk heat capacity of catalyst bed
c_{pf} = specific heat of gas phase
c_{ps} = specific heat of supported catalyst
d_t = diameter of reactor tube
E_i = activation energy for ith reaction
$(-\Delta H_i)$ = heat release associated with ith reaction
k_i = rate constant for ith reaction, having the usual Arrhenius form
K_3 = equilibrium constant for lattice oxygen exchange reaction
L = reactor length

$(L\text{-}O)$ = dimensionless concentration of easily removable oxygen in catalyst lattice
n = number of oxygen atoms consumed by every butene molecule in reaction R1
r_B = rate of butene oxidation
$(S\text{-}O)$ = dimensionless concentration of oxidized sites on catalyst surface
t = time variable
T = temperature
T_o = reactor inlet temperature
T_{ref} = reference temperature
T_w = temperature of reactor coolant
u = superficial fluid velocity
U_h = wall heat transfer coefficient
W_c = weight fraction of active catalyst in supported catalyst
x_B = volume fraction butene in gas phase
z = reactor length variable

Greek letters

λ_{ea} = axial energy dispersion
ρ_f = density of fluid
ρ_s = density of supported catalyst

Literature Cited

Arnold, E. W., "Metal Oxide Catalyzed Partial Oxidation Reactions: The Dynamic Role of Lattice Oxygen and The Effect of Water Vapor on Butane Partial Oxidation," Ph.D. Thesis, Princeton Univ. (1988).

Arnold, E. W., and S. Sundaresan, "The Role of Lattice Oxygen in the Dynamic Behavior of Oxide Catalysts," *Chem. Eng. Commun.*, **58,** 213 (1987).

Blaum, E., "Zur Dynamik des Katalytischen Festbettreaktors bei Katalysator Desaktivierung, I," *Chem. Eng. Sci.*, **29,** 2263 (1974).

Boreskov, G. K., and M. G. Slinko, "Modeling of Chemical Reactors," *Pure Appl. Chem.*, **10,** 611 (1965).

Brazdil, J. F., D. D. Suresh, and R. K. Grasselli, "Redox Kinetics of Bismuth Molybdate Ammoxidation Catalysts," *J. Cat.*, **66,** 347 (1980).

Breckner, E. M., S. Sundaresan, and J. B. Benziger, "Solid Electrolyte Potentiometry Study of Butene Oxidation over Vanadium Phosphate Catalysts," *Appl. Cat.*, **30,** 277 (1987).

Buchanan, J. S., and S. Sundaresan, "Kinetics and Redox Properties of Vanadium Phosphate Catalysts for Butane Oxidation," *Appl. Catal.*, **26,** 211 (1986).

Ervin, M. A., and D. Luss, "Effect of Fouling on the Stability of Adiabatic Packed-Bed Reactors," *AIChE J.*, **16,** 979 (1970).

Gates, B. C., J. R. Katzer, and G. C. A. Schuit, *Chemistry of Catalytic Processes,* McGraw-Hill, New York, 325 (1979).

Hodnett, B. K., and B. Delmon, "Influence of Reductive Pretreatments on the Activity and Selectivity of Vanadium-Phosphorous Oxide Catalysts for *n*-Butane Partial Oxidation," *Ind. Eng. Chem. Fund.*, **23,** 465 (1984).

Liu, S. L., and N. R. Amundson, "Stability of Adiabatic Packed-Bed Reactors. An Elementary Treatment," *Ind. Eng. Chem. Fund.*, **1,** 200 (1962).

Mars, P., and D. W. van Krevelen, "Oxidation Carried Out by Means of Vanadium Oxide Catalysts," *Chem. Eng. Sci.* (*Special Suppl.*), **3,** 41 (1954).

Mehta, P. S., W. N. Sams, and D. Luss, "Wrong-Way Behavior in Packed-Bed Reactors. I: The Pseudohomogeneous Model," *AIChE J.*, **27,** 234 (1981).

Padberg, G., and E. Wicke, "Stabiles und Instabiles Verhalten Eines Adiabatischen Rohrreaktors am Beispiel der Katalytischen Co-Oxydation," *Chem. Eng. Sci.*, **22,** 1035 (1967).

Puszynski, J., and V. Hlavacek, "Experimental Study on Traveling Waves in Nonadiabatic Fixed-Bed Reactors for the Oxidation of Carbon Monoxide," *Chem. Eng. Sci.*, **35,** 1769 (1980).

Razon, L. F., and R. A. Schmitz, "Intrinsically Unstable Behavior During the Oxidation of Carbon Monoxide on Platinum," *Catal. Rev.-Sci. Eng.*, **28,** 89 (1986).

Rhee, H., R. P. Lewis, and N. R. Amundson, "Creeping Profiles in Catalytic Fixed-Bed Reactors. Continuous Models," *Ind. Eng. Chem. Fund.*, **13,** 317 (1974).

Manuscript received Aug. 8, 1988, and revision received Dec. 6, 1988.